JOURNAL OF SOLID STATE CHEMISTRY 45, 119–126 (1982)

Intercalation Phases of TiS_2, 2H–NbS_2, and 1T–TaS_2 with Ethylenediamine and Trimethylenediamine: A Crystal Chemical and Thermogravimetric Study*

H. BOLLER†

Institut für Physikalische Chemie der Universität Wien, Währingerstrasse 42, A-1090 Wien, Austria

AND H. BLAHA

Institut für Anorganische Chemie der Universität Wien, Währingerstrasse 42, A-1090 Wien, Austria

Received February 4, 1982

The title compounds were prepared and chemicaly analyzed. Their crystal structures were determined from rotating crystal photographs. 1T–, 2H–, and two different 3R–polymorphs were observed. The thermogravimetric analysis, revealing two to four distinct steps for the phases derived from TiS_2 and 2H–NbS_2, and only one to two smeared-out steps for those derived from 1T–TaS_2, proves the coexistence of strongly and weakly bound intercalate molecules. The first ones cannot be thermally deintercalated without chemical decomposition. The results are discussed within the framework of an ionic bonding model.

Introduction

Intercalation compounds of transition metal dichalcogenides with organic molecules have been the object of numerous studies (*1*) since their discovery by Weiss and Ruthard (*2*). The main interest of most investigators concentrated on the remarkable physical properties of these substances. Many chemical questions, however, concerning stoichiometry, chemical stability, and bonding are sill insufficiently answered. Few compounds have been well characterized from the crystallographic point of view. This study is an attempt to get more information on these points in the case of the title compounds. Ethylenediamine (en) and trimethylenediamine (tn) were chosen because these amines are easily intercalated forming stable compounds.

Ethylenediamine has already been intercalated in 2H–NbS_2 and 1T–TaS_2 by Schöllhorn *et al.* (*3*). Meyer *et al.* (*4*) report on the preparation and some physical properties of intercalation compounds of ethylenediamine with 2H–TaS_2, 4H–TaS_2, 2H–$NbSe_2$, and 2H–$TaSe_2$. These authors also determined lattice constants and proposed structure models. They remark in a short note that the thermogravimetric analysis indicated partially destructive thermal deintercalation proceeding in several steps within the range of 50–400°C.

* Dedicated to Professor Hans Nowotny.

† Author to whom correspondence should be addressed.

0022-4596/130119-08$02.00/0

Experimental

Sample preparation. The disulfides were prepared from the elements by heating in evacuated sealed off silica tubes to 800°C (1T–TaS_2: 900°C) for several days and subsequent quenching. A sulfur excess of 1% was applied. The products were crystalline (laminas of 0.01–0.3 mm diameter) and single-phase 1T–TiS_2, 2H–NbS_2, and 1T–TaS_2.

The disulfides together with excess amine were vacuum degassed in a closed glass vessel and then heated at 120°C for 20 hr. Already during degassing the amine gets a yellow color, which is darkened during the heating. After decanting the amine one part of the reaction product was washed with ether, the other with warm water until no alkaline reaction was detectable. Both samples were dried in a vacuum desiccator over silica gel.

The intercalation phases show a typical darkening of the color compared with the pure disulfides (e.g., TiS_2 from golden to bronze). Under the microscope the crystals appear swollen perpendicularly to the cleavage planes and loosely composed by warped layers like soaked paste board.

Chemical analyses. The C,H,N,S contents of the starting materials and of most of the reaction and degradation products were determined by microanalysis.[1]

X rays. The products were examined by Debye–Scherrer, rotating crystal, and some Weissenberg photographs. It turned out that rotating crystal photographs around the [001] axis were most useful. Intensities were calculated by the programme PULVROT (5).[2]

Thermogravimetry. The measurements were made by means of a Mettler Thermoanalyzer TA1 in connection with the low-temperature furnace NT, manufactured in quartz. The substance was on a plate-like platinum crucible of 13 mm diameter with a rim of 2.5 mm height. The sample weight varied between 30 and 100 mg according to the molecular weight. The measurements were made under streaming argon (4 liters/hr). The argon was purified from oxygen by a BTS catalyst (column length 1 m, 140°C) and dried over magnesium perchlorate. The heating rate was 1 or 2°/min. After a complete measurement the following runs were interrupted at different temperatures to analyze the sample chemically and by X rays.

[1] We thank Dr. J. Zak, manager of the microanalytic laboratory at the Institut für Physikalische Chemie, for the analyses.

[2] The computer calculations were carried out at the Interuniversitäres Rechenzentrum Wien, Universitätsstrasse.

Results

Chemical Analyses

Typical analyses are compiled in Table I. The C,H,N values, like the C : H and C : N ratios of different preparations, scatter somewhat. The C : N ratios are almost always higher than those calculated. Apparently there are side reactions during intercalation. The C : H ratios are generally too small, especially in samples washed with water, indicating water uptake.

Therefore these intercalation phases are chemically not very well defined, and the specification of the intercalate content is only approximative, depending on the manner of its calculation. The x values given in Table II were calculated on the basis of the nitrogen contents. The chemical analyses prove that a part of the amine is washed out by water.

Crystal Structures

Since the crystals are composed of more or less warped lamellas, the X-ray reflections on the rotation diagrams are somewhat extended along the ζ coordinate. The intensities fall off rather rapidly at higher angles because of disturbed long-range order. Therefore it is not possible to deter-

TABLE I

CHEMICAL ANALYSES OF REPRESENTATIVE SAMPLES (wt%)

	T^a (°C)	C	H	N	S
TiS_2					56.70
$TiS_2 \cdot$ en a[b]		7.74	2.54	8.01	44.02
	400	3.91	0.64	1.67	51.28
$TiS_2 \cdot$ en b		4.91	2.03	4.87	46.20
	180	4.22	1.91	4.80	48.02
	280	4.37	1.18	2.42	50.73
	340	3.86	0.84	1.37	51.62
	400	3.09	0.53	1.15	51.73
NbS_2		—	—	—	41.5
$NbS_2 \cdot$ en a		4.28	1.67	5.06	34.95
$NbS_2 \cdot$ en b		3.36	1.58	3.87	35.46
	340	2.69	0.23	0.86	37.61
TaS_2		—	—	—	26.52
$TaS_2 \cdot$ en a		3.37	1.15	3.80	23.71
$TaS_2 \cdot$ en b		1.71	0.66	1.90	24.69
	560	0.89	0.10	0.34	23.85
$TiS_2 \cdot$ tn a		8.69	2.51	6.20	41.82
$TiS_2 \cdot$ tn b		5.95	2.11	3.69	42.50
$NbS_2 \cdot$ tn a		5.98	1.77	4.53	35.22
$NbS_2 \cdot$ tn b		5.25	1.67	3.86	35.39
$TaS_2 \cdot$ tn a		4.33	1.22	3.31	23.29
$TaS_2 \cdot$ tn b		2.22	0.73	1.74	23.86

[a] The temperatures refer to samples drawn from the TGA.

[b] a = sample washed with ether. b = sample washed with water.

mine the lattice constants and intensities with great accuracy. On the other hand the determination of the c parameter is facilitated by the presence of (00l) reflections on the rotation diagrams. These reflections are sharp as far as they belong to the basic pattern. In addition some crystals also show diffuse reflections or bands along the (00ζ) direction, indicating disordered portions with different periodicity. Sometimes the intercalation phase is associated with unchanged disulfide. Especially the rhombohedral polytypes show intergrowth with unreacted 1T-disulfide in such a manner that the ratio c_{3R}/c_{1T} is almost exactly 5, although the c/a ratios of 1T-TiS_2 and 1T-TaS_2 are different.

Structure models for the intercalation phases can be worked out from the unit cells assuming that the TS_2 slabs, staying essentially unchanged on intercalation, are shifted parallel to each other by vectors (00δ/c) or $\pm$ ($\frac{1}{3}$, $\frac{2}{3}$, δ/c), δ being the increase of interlayer separation. The sulfur atoms of the neighboring layers are lying either one above the other or in staggered position.

The crystallographic data of the prepared phases are compiled in Table II, and the observed polytypes are depicted schematically in Fig. 1. Tables III–V compare observed and calculated intensities of the rotation diagrams.

The intercalation phases of ethylenediamine with 1T-TaS_2 occur in two modifications with almost the same unit cell. The sulfur atoms lie either one above the other (3R′) or staggered (3R). The 3R modification, corresponding to a larger intercalate content ($x \approx 0.36$) is observed in products washed with ether. This polytype has already been described by Meyer *et al.* (*4*), assigning to it, however, a smaller $x = 0.25$. The 3R′ modification containing less ethylenediamine ($x \approx 0.17$) is observed after washing with water or after partial thermal deintercalation. Some crystals, however, were found in samples washed with ether, whose X-ray diagrams indicate coexistence of both stacking modes.

The trimethylenediamine complexes of 1T-TaS_2 are also dimorphous. The crystal structure of samples washed with ether is complex, with a superstructure in the (001) plane.

The 1T polymorph of $TiS_2 \cdot tn_x$ seems to be metastable, because its powder pattern is changed after grinding. An indexation of the new pattern was not possible.

The rotation diagrams of $NbS_2 \cdot en_x$ show alternating sharp ($l = 2n$) and diffuse ($l = 2n + 1$) layer lines. This is obviously caused by neighboring NbS_2 slabs having the same orientation. In the ideal structure such slabs

TABLE II

INTERCALATION PHASES WITH ETHYLENEDIAMINE AND TRIMETHYLENEDIAMINE[a]

	a (Å)	c (Å)	δ (Å)	x_1	x_2	Max. packing density in %	Polytype
$TiS_2 \cdot en_x$	3.415	28.58	3.83	0.39	0.21	75	3R′
$NbS_2 \cdot en_x$	3.341	18.64	3.38	0.32	0.24	72	2H′
$TaS_2 \cdot en_x$	3.372	29.32	3.87	0.36	0.17	70	3R, 3R′
$TiS_2 \cdot tn_x$	3.42	9.82	4.12	0.33	0.15	70	1T
$NbS_2 \cdot tn_x$	3.34	18.73	3.42	0.29	0.24	78	2H′
$TaS_2 \cdot tn_x$	3.38	29.09	3.80	0.32	0.16	76	3R′[b]

[a] The stoichiometric parameters x_1 and x_2 refer to samples washed with ether and washed with water, respectively. They are calculated from the nitrogen contents. The lattice constants refer to samples washed with water ($x = x_2$).

[b] Only samples washed with water ($x \approx 0.16$).

are rotated by 180°. Stacking faults of that kind reduce locally the c axis periodicity to one-half. As a consequence they give rise to the broadening of the reflections with odd l. 2H–NbS_2 itself cannot be prepared without the same type of stacking faults[3] (*6*). They stay unchanged on intercalation, because a recovery would require the rotation of a whole slab.

Even strongly exposed Weissenberg films did not show superstructure reflections caused by intercalate ordering. The increase of interlayer separation δ ranging between 3.4 and 4.1 Å (Table II) suggests a monomolecular layer of organic molecules with their chain axis essentially parallel to the TS_2 slabs. δ is almost independent of the intercalate content. There is a slight increase of the a axis parameters on intercalation.

[3] In this case reflections with $h - k \neq 3n$ are diffuse because of the different polytype.

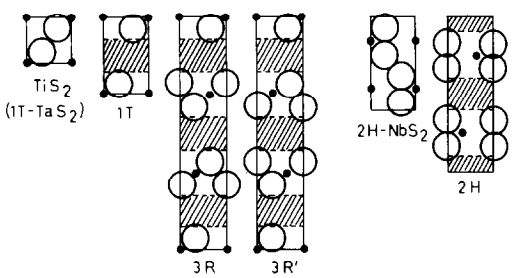

FIG. 1. The structures of the intercalation phases (section through (110) plane).

Thermogravimetry

$TiS_2 \cdot en_x$. The product washed with ether (Fig. 2, curve *a*) loses predominantly weakly bound ethylenediamine (bp. = 116°C) in two first steps between 100 and 200°C without structural change of the 3R polytype. Then the intercalation phase is decomposed in another two steps leading via an intermediate phase (β) to the lattice of TiS_2. Curve *b* reveals in agreement with the chemical analysis that washing with water removes most of the loosely bound amine replacing it partially by water. It was not possible to index the rotation diagram of the β phase because of the poor quality of the crystals. The chemical analyses prove that the deintercalation is accompanied by pyrolysis and sulfur loss. The latter is the probable reason for a somewhat smaller c parameter of the resulting TiS_2 compared with normal titanium disulfide. After deintercalation all products contain considerable amounts of carbon and less nitrogen, which are not substantially diminished even at 500°C (Table I). The volatile pyrolytic products or sulfur deposit as

TABLE III

INTENSITIES OF ROTATION DIAGRAMS OF THE 3R POLYMORPHS (SPACE GROUP: $R\bar{3}m$–D_{3d}^5; 3 T IN (3*a*) 000; 6 S IN (6*c*) 00*z*

	3R′–$TiS_2 \cdot en_x$ $z = 0.387$		3R′–$TaS_2 \cdot en_x$ $z = 0.390$		3R – $TaS_2 \cdot en_x$ $z = 0.720$	
(*hkl*)	I_o	I_c	I_o	I_c	I_o	I_c
(110)	mst	70	st	72	mst	76
(300)	mw	24	m	29	mw	30
(220)	m	32	m	43	mw	45
(101)	—	0	m	29	mst	53
(021)	—	0	vw	8	mw	13
(211)	—	0	vw	9	mw	15
(131)	—	0	—	18	—	30
(012)	mw	30	mst	66	mw	25
(202)	vw	6	w	17	—	7
(122)	vw	6	w	19	—	8
(312)	—	10	mw	38	—	17
(113)	m	37	mst	54	mst	59
(303)	vw	12	mw	22	mw	24
(223)	—	17	mw	34	mw	37
(104)	vw	3	mw	23	vst	95
(024)	st	100	vvw	7	mw	23
(214)	mw	21	vvw	8	m	28
(134)	mw	24	—	18	m d	62
(015)	m	46	vst	100	m	28
(205)	vw	2	mw	25	w	8
(125)	vw	7	mw	30	—	10
(315)	st	78	m	73	—	23
(116)	vw	2	mw	26	m	30
(306)	—	0	vw	11	w	13
(226)	—	0	—	20	—	23
(107)	vw	7	m	47	vst	100
(027)	—	2	vw	13	m	26
(217)	—	2	vvw	16	m	32
(018)	st	78	st	80	mst	55
(208)	w	18	w	21	mw	15
(128)	w	22	w	27	mw	19
(119)	—	1	w	16	mw	17
(309)	—	1	—	8	—	9
(10.10)	mst	59	st	79	st	62
(02.10)	w	15	mw	22	—	18
(21.10)	w	19	mw	30	—	24
(01.11)	mw	14	mst	39	st	85
(20.11)	vw	3	w	11	m	24
(12.11)	—	2	w	16	—	35
(11.12)	—	0	mw	26	m	23
(30.12)	—	0	—	18	—	16
(10.13)	st	83	mst	82	m	31
(02.13)	w	22	w	24	—	5
(21.13)	—	33	w	37	—	14

small amounts of yellow substance at the cooler parts of the furnace.

$NbS_2 \cdot en_x$. The amount of loosely bound intercalate is somewhat less in $NbS_2 \cdot en_x$ than in $TiS_2 \cdot en_x$ (Fig. 3, curve *a*). The decomposition starts from 200°C onwards in two steps. The degradation after washing

TABLE IV

INTENSITIES OF A ROTATION DIAGRAM OF $NbS_2 \cdot en_x$ (SPACE GROUP: $P6_3mmc$–D_{6h}^4; 2 Nb IN (2*c*) $\frac{1}{3}, \frac{2}{3}, \frac{1}{4}$; 4 S IN (4*e*) 00*z*, $z = 0.170$)

(*hkl*)	I_o	I_c	(*hkl*)	I_o	I_c	(*hkl*)	I_o	I_c
(100)	w	4	(222)	mst	33	(106)	vst	100
(110)	st	81	(312)	—	1	(116)	w	4
(200)	—	0	(103)	mst d	64	(206)	m	26
(210)	—	1	(203)	mw d	15	(216)	m	35
(300)	mst	31	(213)	mw d	18	(306)	—	2
(220)	st	48	(313)	m d	47	(226)	w	5
(310)	—	2	(104)	st	51	(107)	m	53
(101)	mst d[a]	68	(114)	mw	15	(207)	mw	15
(201)	mw d	16	(204)	mw	12	(217)	mw+	20
(211)	m d	18	(214)	mw	15	(108)	st	59
(311)	mst d	37	(304)	w	6	(118)	m−	9
(102)	—	1	(224)	mw	11	(208)	m	16
(112)	st	53	(314)	st	57	(218)	m+	26
(202)	—	0	(105)	mst d	58	(308)	w	6
(212)	—	0	(205)	mw d	15			
(302)	m	21	(215)	mw+d	18			

[a] d = diffuse. The intensities of these reflections are always underestimated.

with water proceeds similarly to the analogous TiS_2 derivative (curve *b*). In particular, the first step (predominantly water discharge), corresponding to approximately the same molar amounts for both phases (1.8 versus 2.5%), is very flat in the region from 160 to 200°C. In both cases the proper decomposition (first decomposition step) starting at about 210°C and ending at 270–290°C is followed by a second step. Unlike

TABLE V

INTENSITIES OF A ROTATION DIAGRAM OF $TiS_2 \cdot tn_x$ (SPACE GROUP: $P\bar{3}m1$–D_{3d}^3; 1 Ti IN (1*a*) 000; 2 S IN (2*d*) $\frac{1}{3}, \frac{2}{3}, z$, $z = 0.155$)

(*hkl*)	I_o	I_c	(*hkl*)	I_o	I_c	(*hkl*)	I_o	I_c
(100)	ww	3	(301)	w	12	(113)	—	1
(110)	mst	67	(221)	mw	17	(203)	mw	21
(200)	—	1	(311)	m	21	(213)	mw	26
(210)	—	1	(102)	st	100	(303)	—	0
(300)	mw	23	(112)	vw	3	(223)	—	2
(220)	m	31	(202)	mw	22	(104)	mst	83
(310)	—	1	(212)	mw	25	(114)	—	0
(101)	st	54	(302)	—	1	(204)	mw	21
(111)	m	37	(222)	—	1	(214)	mw	29
(201)	w	11	(312)	m	55	(304)	—	0
(211)	w	12	(109)	st	90			

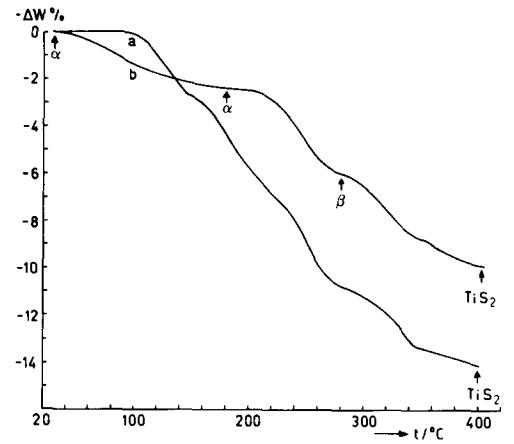

FIG. 2. Thermograms of $TiS_2 \cdot en_x$ (explanation in the text).

titanium disulfide weight constancy is almost reached between 350 and 480°C because of less sulfur loss. Again the chemical analyses show that an important part of the original carbon, and less nitrogen and hydrogen, are retained. X rays show that the 2H′ modification (α) stays unchanged until about 200°C. After the first decomposition step rather diffuse patterns are observed (β), indicating the transformation to 2H–NbS_2, which is the end product after the second decomposition step (~400°C). Also in this case the c parameter is somewhat smaller than that of pure 2H–NbS_2.

$TaS_2 \cdot en_x$. The thermograms of $TaS_2 \cdot en_x$ (Fig. 4) are less articulated than the preceding ones. Only two steps can be

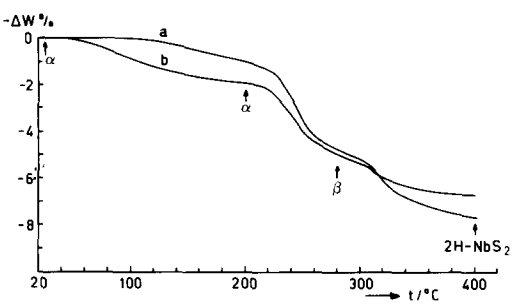

FIG. 3. Thermograms of $NbS_2 \cdot en_x$ (explanation in the text).

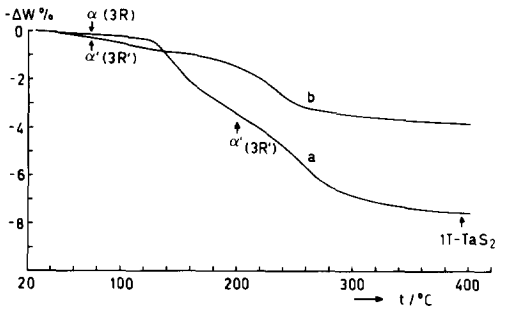

FIG. 4. Thermograms of $TaS_2 \cdot en_x$ (explanation in the text).

recognized in curve a (blurred point of inflexion at about 200°C). The degradation of the intercalation phase is already finished after the first decomposition step gradually starting at about 160°C and ending at 290°C. Thus there is no second decomposition step. The thermograms of the products washed with water (Fig. 4, curve b) indicate predominant loss of water until about 120°C. The following decomposition step is substantially flatter and about 20°C earlier at the end. The powder diagrams of samples washed with water, unlike those of samples washed with ether, always show variable amounts of 1T–TaS_2. Apparently also a portion of more strongly bound ethylenedi-

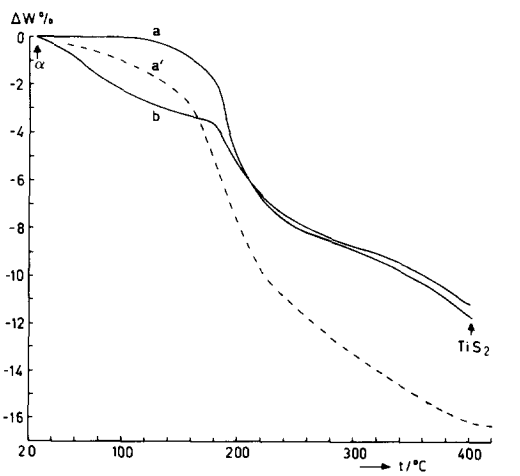

FIG. 5. Thermograms of $TiS_2 \cdot tn_x$ (explanation in the text).

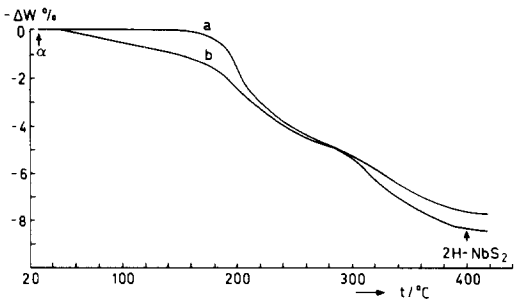

FIG. 6. Thermograms of $NbS_2 \cdot tn_x$ (explanation in the text).

amine is washed out. X rays also show that the 3R polytype (α) of the product washed with ether is transformed to the 3R′ polytype (α') before being decomposed to 1T–TaS_2, which contains less residue of organic material, probably because of the lower thermal stability of the intercalation phase.

The intercalation phases with trimethylenediamine. The thermograms of these phases are very similar to those of the ethylenediamine complexes, (Figs. 5–7). There is again a loosely bound fraction of intercalate, which can be washed out or be partially replaced by water, and a tightly bound one. Additional water uptake is also possible in $TiS_2 \cdot tn_x$, as is shown from curve *c*, Fig. 5, taken from the same substance as curve *a* after several weeks in air. The discharge of the tightly bound fraction proceeds in the cases of $TiS_2 \cdot tn_x$ and $NbS_2 \cdot tn_x$ again in two, yet less distinct decomposition steps, while the thermogram of

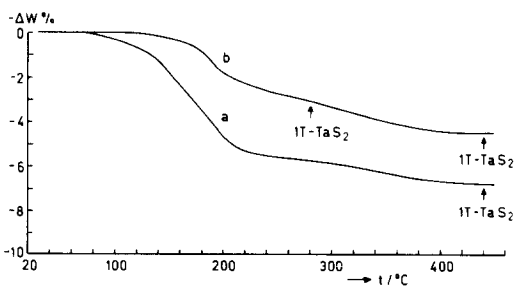

FIG. 7. Thermograms of $TaS_2 \cdot tn_x$ (explanation in the text).

$TaS_2 \cdot tn_x$ is hardly articulated, taking throughout a flatter course after washing with water.

The discharge of the loosely bound fraction and the first decomposition step generally set in 20–30°C earlier than in the ethylenediamine compounds.

Conclusions

From the TGA measurements, together with the chemical analyses, it can be concluded that there are two types of organic intercalate molecules. One part is chemically tightly bound, the other one forms a solvate. The solvate molecules can be washed out and partially replaced by water without substantial change of the increase of interlayer separation δ. The proper decomposition, setting in at about 200°C (en) and 180°C (tn), proceeds in the case of the TiS_2 and 2H–NbS_2 derivatives in two steps, suggesting formation of a higher-stage intercalation phase (e.g., second stage for $TiS_2 \cdot en_x$). Although rotating crystal diagrams indicate indeed an intermediate crystallographically distinct modification, it should be borne in mind that according to the chemical analyses the products are chemically ill defined, the degradation being accompanied by pyrolytic decomposition of the intercalate and sulfur loss. Even after complete thermal deintercalation the samples contain considerable amounts of carbon together with less nitrogen and little hydrogen. It seems that a large portion of the tightly bound organic molecules are thermally dehydrogenated (perhaps sulfodehydrogenation).

These findings prove that the thermal deintercalation of the title phases is not at all reversible, not even with respect to the disulfide.

The thermal stabilities of the TiS_2 and 2H–NbS_2 derivatives are comparable, while the 1T–TaS_2 derivatives are less stable.

The 2H′ polymorph has already been observed in various intercalation phases derived from 2H dichalcogenides. On the contrary, the crystal structures of the 1T derivatives show a greater variety than expected. The existence of a 1T polymorph ($TiS_2 \cdot tn_x$)[4] is especially interesting, because it restricts the general validity of the rule 1T → 3R on intercalation. The observed polymorphs differ either in the relative position of neighboring sulfur layers (one above the other in 3R′, 2H′, and staggered in 1T or 3R) or in the stacking of the TS_2 slabs (3R and 3R′ or 1T). The factors responsible for the latter differences do not show up in the thermogravimetric behavior. There are, however, remarkable differences in the increase of interlayer separation δ, being largest in the 1T polytype. They are, perhaps, connected with the conformation of the intercalated molecules. On the other hand, the 3R(R′) polymorphs might be stabilized by intergrowth with unchanged 1T disulfide. The δ are on the order of magnitude of the thickness of the molecules lying between the layers. The maximum packing densities φ are calculated according to

$$\varphi = x_1 \frac{V_{\text{molecule}}}{V_{\text{interlayer}}} \cdot 100 = \frac{2}{3^{1/2}} x_1 \frac{V_{\text{molecule}}}{a^2 \cdot \delta} \cdot 100,$$

estimating the molecular volumes from volume increments (*7*). The values given in Table II are calculated (en: 74 Å³; tn: 89 Å³). They range between 70 and 78%, which is typical for close packing of organic molecules.

The great thermal stability and the irreversibility of the thermal deintercalation suggest that at least in the case of the phases derived from TiS_2 and 2H–NbS_2 the ionic bonding model is more probable than the charge transfer model. Such an ionic model has been proposed by Schöllhorn and Zagefka for $TaS_2 \cdot NH_3$ (*8*) and by Schöllhorn *et al.* for $TaS_2 \cdot py_{1/2}$ (*9*). Accordingly the phases should be formulated as

$$TS_2^{x-} \cdot (RH^+)_x \cdot R_y \cdot (X, H_2O)_z,$$

R symbolizing the organic amine and *X* different cointercalated oxidation products, originating from internal redox reactions, which produce the ammonium ions. The chemical analyses (too high C:N ratios) and the yellow color of the excess amine after the intercalation reaction, which is not due to dissolved sulfur, suggest side reactions of this kind.

Accordingly, the intercalation phases are typical nonstoichiometric systems, which are chemically badly defined with respect to the intercalate. The total amount of intercalate is mainly governed by the space requirements of the molecules, while the tightly bound fraction is determined by the redox potential of the system.

[4] Orienting experiments showed another 1T polytype in the case of $TiSe_2 \cdot en_x$ with $a = 3.56, c = 10.04$, and $\delta = 4.4$ Å.

References

1. G. V. Subba Rao and M. W. Shafer, "Intercalated Layered Materials" (F. A. Levy, Ed.), p. 99, Reidel, Dordrecht, 1979.
2. A. Weiss and R. Ruthard, *Z. Naturforsch. B* **24,** 356 (1969).
3. R. Schöllhorn, E. Sick, and A. Weiss, *Z. Naturforsch. B* **28,** 168 (1979).
4. S. F. Meyer, R. E. Howard, G. R. Stewart, J. V. Acrivos, and T. H. Geballe, *J. Chem. Phys.* **62,** 4411 (1975).
5. H. Boller, unpublished. Program PULVROT, written in FORTRAN IV for the calculation of angles and intensities of X-ray and neutron powder and rotating crystal diagrams.
6. F. Jellinek, *Ark. Kemi* **20** (36), 454 (1963).
7. A. I. Kitaigorodsky, "Molecular Crystals and Molecules," p. 20, Academic Press, New York/London, 1973.
8. R. Schöllhorn and H. D. Zagefka, *Angew. Chem.* **89,** 193 (1977).
9. R. Schöllhorn, H. D. Zagefka, T. Butz, and A. Lerf, *Mater. Res. Bull.* **14,** 369 (1979).